

How the insulating properties of snow affect soil carbon distribution in the continental pan-Arctic area

I. Gouttevin,^{1,2} M. Menegoz,^{2,3} F. Dominé,^{2,4} G. Krinner,² C. Koven,⁵ P. Ciais,³ C. Tarnocai,⁶ and J. Boike⁷

Received 1 December 2011; revised 31 March 2012; accepted 11 April 2012; published 2 June 2012.

[1] We demonstrate the effect of an ecosystem differentiated insulation by snow on the soil thermal regime and on the terrestrial soil carbon distribution in the pan-Arctic area. This is done by means of a sensitivity study performed with the land surface model ORCHIDEE, which furthermore provides a first quantification of this effect. Based on field campaigns reporting higher thermal conductivities and densities for the tundra snowpack than for taiga snow, two distributions of near-equilibrium soil carbon stocks are computed, one relying on uniform snow thermal properties and the other using ecosystem-differentiated snow thermal properties. Those modeled distributions strongly depend on soil temperature through decomposition processes. Considering higher insulation by snow in taiga areas induces warmer soil temperatures by up to 12 K in winter at 50 cm depth. This warmer soil signal persists over summer with a temperature difference of up to 4 K at 50 cm depth, especially in areas exhibiting a thick, enduring snow cover. These thermal changes have implications on the modeled soil carbon stocks, which are reduced by 8% in the pan-Arctic continental area when the vegetation-induced variations of snow thermal properties are accounted for. This is the result of diverse and spatially heterogeneous ecosystem processes: where higher soil temperatures lift nitrogen limitation on plant productivity, tree plant functional types thrive whereas light limitation and enhanced water stress are the new constraints on lower vegetation, resulting in a reduced net productivity at the pan-Arctic scale. Concomitantly, higher soil temperatures yield increased respiration rates (+22% over the study area) and result in reduced permafrost extent and deeper active layers which expose greater volumes of soil to microbial decomposition. The three effects combine to produce lower soil carbon stocks in the pan-Arctic terrestrial area. Our study highlights the role of snow in combination with vegetation in shaping the distribution of soil carbon and permafrost at high latitudes.

Citation: Gouttevin, I., M. Menegoz, F. Dominé, G. Krinner, C. Koven, P. Ciais, C. Tarnocai, and J. Boike (2012), How the insulating properties of snow affect soil carbon distribution in the continental pan-Arctic area, *J. Geophys. Res.*, 117, G02020, doi:10.1029/2011JG001916.

¹École Nationale du Génie Rural, des Eaux et des Forêts, AgroParisTech, Paris, France.

²Laboratoire de Glaciologie et Géophysique de l'Environnement, UMR5183, CNRS/Université Joseph Fourier–Grenoble, Grenoble, France.

³CEA/CNRS/UVSQ, LSCE, Saclay, France.

⁴Takuvik Joint International Laboratory, Université Laval (Canada) and CNRS (France), Québec City, Québec, Canada.

⁵Lawrence Berkeley National Laboratory, Berkeley, California, USA.

⁶Research Branch, Agriculture and Agri-Food Canada, Ottawa, Ontario, Canada.

⁷Alfred Wegener Institute for Polar and Marine Research, Potsdam, Germany.

Corresponding author: I. Gouttevin, CNRS/Université Joseph Fourier–Grenoble 1, LGGE UMR5183, BP 96, 54, rue Molière, FR-38402 Saint-Martin d'Hères, France. (isabelle.gouttevin@lgge.obs.ujf-grenoble.fr)

Copyright 2012 by the American Geophysical Union.
0148-0227/12/2011JG001916

1. Introduction

[2] Recent estimates highlight the importance of the northern circumpolar soil organic carbon reservoir [Zimov *et al.*, 2006; Tarnocai *et al.*, 2009; Schirrmeister *et al.*, 2011], which could amount to up to 1672 PgC and thus outweigh the vegetation (~700 PgC) and atmospheric (~750 PgC) carbon pools together. Most of this carbon is stored in frozen soils and undergoes very slow or no microbial decomposition due to low temperatures [Zimov *et al.*, 2006]. However, the labile fraction of this long-lived soil carbon pool could be subject to severe degradation as climate warms at high latitudes, primarily due to enhanced soil respiration as temperature increases, wetland formation and disappearance, thermokarst formation and fires [Gruber *et al.*, 2004; Christensen *et al.*, 2004; Davidson and Janssens, 2006; Schuur *et al.*, 2008, 2009]. Part of the high latitudes soil carbon could then be released to the atmosphere in the form CO₂ or methane, greenhouse gases providing

a positive feedback to global warming [e.g., Zhuang *et al.*, 2006; Khvorostyanov *et al.*, 2008; Koven *et al.*, 2011].

[3] Accounting for the soil carbon pool and its lability in global climate models is paramount to improve the accuracy of climate projections [Randall *et al.*, 2007]; it is all the more crucial in the Arctic as the strongest warming is projected for those regions [Meehl *et al.*, 2007]. However, soil carbon dynamics results from a variety of intricate and complex processes [e.g., Davidson and Janssens, 2006], which coupled climate-carbon cycle models still struggle to capture with accuracy [Friedlingstein *et al.*, 2006; Schaphoff *et al.*, 2006]. Snow cover dynamics is one of them: the insulating properties of snow [e.g., Dominé *et al.*, 2007; Zhang, 2005] strongly modulate the soil thermal regime [Westermann *et al.*, 2009; Qian *et al.*, 2011] and hence affect soil carbon dynamics at high latitudes [Walker *et al.*, 1999; Nobrega and Grogan, 2007]. In particular, winter below-snow soil carbon activity has long been reported [Kelley *et al.*, 1968; Zimov *et al.*, 1993] with a significant contrast between tundra and taiga ecosystems [Sullivan *et al.*, 2008; Sullivan, 2010] in link with the snow cover.

[4] The insulating properties of snow depend on snow depth and snow thermal conductivity. However, this last variable is poorly represented in land surface models designed for large-scale applications. Often, only snow depth is considered, and when thermal conductivity is included, it is indirectly through its relationship with snow density ρ [Zhang, 2005; Ling and Zhang, 2006; Lawrence and Slater, 2010]. The compilation by Sturm *et al.* [1997] shows that a rather loose correlation exists between ρ and thermal conductivity k_{eff} . For example, Sturm *et al.* [1997, Figure 6] show that for $\rho = 0.29 \text{ g cm}^{-3}$, k_{eff} values range from 0.04 to $0.22 \text{ W m}^{-1} \text{ K}^{-1}$, and this spread of k_{eff} values is observed throughout the range of snow ρ values. This is because k_{eff} depends on climatic conditions, and especially on local wind conditions. In the taiga, snow is sheltered from wind effects by vegetation, so that depth hoar of low k_{eff} forms [Sturm and Johnson, 1992]. On the tundra, wind compaction of snow leads to hard windpacks [Dominé *et al.*, 2002] of high k_{eff} in the upper part of the snowpack [Sturm *et al.*, 1997]. Basal depth hoar also forms on the course of the snow season [Derksen *et al.*, 2009] but the tundra snowpack remains overall more conductive than taiga snow [Sturm *et al.*, 1995, 2001a].

[5] The goal of this study is to evaluate the sensitivity of soil carbon stocks and dynamics to ground insulation by snow, by means of terrestrial soil carbon modeling. More precisely, we aim at quantifying the impact of the difference in snow thermal properties between taiga and tundra environments. We therefore performed measurements of ρ and k_{eff} in typical taiga and tundra environments. Measuring ρ is useful because for a given snow mass above ground, it determines snowpack height, h , an important factor in computing the thermal resistance of the snowpack $R = h/k_{\text{eff}}$. We then numerically computed the pan-Arctic soil carbon stocks using either a uniform snow conductivity and density (which corresponds to the default settings of our model, and reflects thermal properties very close to a tundra snowpack), or an ecosystem-type-dependent snow conductivity and density, in agreement with our measurements. Spatially explicit soil carbon accumulation in the Arctic is simulated by the land-surface model ORCHIDEE [Krinner *et al.*, 2005] run in off-line mode. Many studies have now investigated the influence

of snow on the soil thermal regime and carbon dynamics at the point scale, both in winter and over the whole year [e.g., Welker *et al.*, 2000; Nobrega and Grogan, 2007; Sullivan, 2010]. To our knowledge, it is however the first study aiming at quantifying this impact on the soil carbon dynamics and stocks at the pan-Arctic scale. The discussion focuses on the comparison of both soil carbon distributions and the understanding of the processes driving the major changes in the soil carbon dynamics at the instance of soil thermal regime, net primary production, respiration rate and active layer thickness.

2. Experimental and Modeling Methods

[6] Snow ρ and k_{eff} vertical profiles were measured in the taiga of Finnish Lapland near Sodankylä ($67^{\circ}25'N$, $25^{\circ}35'W$) and on the tundra near Barrow, on the Alaska Arctic coast ($71^{\circ}19'N$, $156^{\circ}39'W$). In both cases, several sites were studied to ensure local spatial representativeness. Density was measured using standard density cutters and a field scale, while k_{eff} was measured using the heated needle probe method [Morin *et al.*, 2010].

[7] The model used for the computation of the spatially explicit soil carbon stocks in the pan-Arctic is the ORCHIDEE model [Krinner *et al.*, 2005], with no dynamic vegetation. This model computes the biomass and soil carbon dynamics as a response to a prescribed climate: soil carbon formation results from the balance between litterfall (input) and decomposition losses (outputs), which are controlled by vegetation growth, productivity, senescence, and soil thermal and hydrological conditions. Fire disturbance is also accounted for. Autotrophic and heterotrophic respirations are temperature dependant; the effect of freeze-induced inhibition on heterotrophic respiration is parametrized using Q10 values of 10^4 below the freezing point and 2 above the freezing point [Koven *et al.*, 2011]. Plant productivity can be affected by light, water and nitrogen limitations, the latter being temperature and moisture dependant [Friedlingstein *et al.*, 1999]. The snow model is quite coarse, with a unique and homogeneous snow layer evolving as a result of snowfall, sublimation and melt. Snow aging is parameterized through an exponential decrease of albedo with time [Chalita, 1992]. Canopy interception, liquid water in snow, and refreezing of this water, are not considered. From a thermal point of view, snow is characterized by a fixed bulk density and thermal conductivity; however, heat diffusion in the snowpack is vertically discretized over 7 layers [Koven *et al.*, 2009].

[8] We use the version of ORCHIDEE modified by Koven *et al.* [2009] to include additional soil carbon processes specific of cold regions: the soil organic matter input and decomposition processes are vertically resolved; cryoturbation and insulation by organic matter are represented; anoxic decomposition and moisture-dependent diffusion of oxygen and methane in soils are accounted for. A detailed representation of these processes is particularly crucial in the pan-Arctic area due to the magnitude of the soil carbon stocks involved and to the high sensitivity of the decomposition processes to temperature around the freezing point [Davidson and Janssens, 2006], which is reached in summer in the upper soil of permafrost regions and at the permafrost margins.

[9] In this study, the spatially explicit soil carbon stocks in the pan-Arctic are computed by ORCHIDEE as in near-

Table 1. Snow Density and Thermal Conductivity Values Used in the CTRL and VARIED Simulations

Simulation	Snow Type	Snow Density (kg/m ³)	Snow Thermal Conductivity (W/m/K)
CTRL	Tundra	330	0.2
	Taiga	330	0.2
VARIED	Tundra	330	0.25
	Taiga	200	0.07

equilibrium with present-day climate and vegetation. By *near-equilibrium* we mean that their evolution is less than 1% year-to-year change in carbon storage. It is achieved after at least 10,000 years of soil carbon computation forced by the climate of random years of the period 1900–1910. Today's soil carbon stocks can be considered in equilibrium with the current climate in regions where the soil carbon decomposition time is short when compared to the centennial time scale. The tropical regions illustrate this situation. In Arctic regions however, due to the low temperatures, the soil carbon decomposes over millennial time scales [Schirmer et al., 2002; Zimov et al., 2006]. A realistic computation of present-day soil carbon stocks would require a detailed representation of the biosphere and climate history over at least the past 10,000 years, in addition to the representation of diverse pedogenic processes (eolian, alluvial, limnic deposition, erosion, carbon export...). Climate modeling over this time scale is both still highly uncertain and computationally expensive [Ganopolski et al., 1998]. This difficulty is overcome by some modeling groups [Kleinen et al., 2010], who make use of the monthly climatology simulated by an Earth Model of Intermediate Complexity (EMIC) superimposed on the twentieth-century climate, and of a dynamic vegetation model (DVG), to trace back the evolution of the biosphere and soil carbon from the past 8000 years onward. However, this approach is not free of uncertainties largely due to the poor constraints on EMICs and dynamic vegetation models [Petoukhov et al., 2000] and it requires the use of several complex tools. We intend to point out and describe the sensitivity of the pan-Arctic soil carbon stocks to insulation by snow: this sensitivity approach lessens the concern of a faithful representation of the soil carbon stocks with respects to current in situ estimates, and justifies our simplified methods. The use of the 20th century climatology is similarly objectionable due to the warming experienced at high latitudes, but proceeds from the same motivation. The meteorological forcing we used is the CRUNCEP data set developed by N. Viovy (url: <http://dods.extra.cea.fr/data/p529viovy/cruncep/readme.htm>). It combines the CRU-TS2.1 [Mitchell and Jones, 2005] monthly climatology covering the period 1901–2002, with the NCEP reanalyses starting from 1948. The details of this forcing can be found at the above-cited URL. We also used a constant atmospheric CO₂ concentration of 350 ppm for the whole simulations.

[10] The procedure used for our soil carbon stocks computation is the following. Phase 1: The model is first run over 100 years randomly taken from the 1901–1910 period to reach the thermal and hydrological equilibrium of the soil and vegetation system. Such a long spinup is required because the soil thermal dynamics is computed over 50 m depth [Alexeev et al., 2007]. Phase 2: Then, a simplified soil

carbon module of ORCHIDEE is used to compute the soil carbon dynamics resulting from this 1901–1910 equilibrium state. This simplified soil carbon module uses the net primary production (NPP) calculated at the end of phase 1 to build soil carbon stocks over centennial timescales. However, the amount of carbon in the soil will affect the full ORCHIDEE equilibrium state. An example of this feedback is the thermal insulation provided by organic matter, which impacts the soil thermal properties and state, with implications for the soil carbon decomposition. Therefore, the simplified soil carbon module cannot be run indefinitely uncoupled from the full ecosystem model, which must be switched on during short phases to reach a new thermal and hydrological equilibrium for the soil and vegetation system. As the new equilibrium state is not very far from the initial one, the re-equilibration phases can be shorter than phase 1. We chose to intertwine periods of 1000 years of exclusive offline soil carbon spinup with short 5-year re-equilibration phases of the full ecosystem model. The spinup plus re-equilibration phases are iterated 10 times to finally achieve a 10,000-year soil carbon spinup consistent with the 1901–1910 climatology. Phase 3: A full ORCHIDEE run over the 1901–2000 time period is carried out, starting with the model in equilibrium with the 1901–1910 climate and soil carbon stocks built over 10,000 years. This simulation is designed to represent the twentieth-century evolution of the soil and vegetation system, including carbon stocks.

[11] The above mentioned procedure is used for a set of two simulations. The first simulation (CTRL) uses of a uniform and constant snow conductivity and density, as prescribed in the default setting of ORCHIDEE. These default snowpack properties are very close to the properties of tundra snow (see Table 1). They lead to a first distribution of equilibrated soil carbon reservoirs, fluxes, and biomass over the continental pan-Arctic area for the twentieth century. In the second simulation (VARIED), we implemented a snow thermal conductivity and density dependent on the vegetation cover, with values derived from our field measurements. The values used for the densities and thermal conductivities in the two simulations are listed in Table 1. The criterion we use to distinguish taiga from tundra environments is based on vegetation types: tree or shrub-like vegetation is assigned taiga characteristics; tundra environments encompass lower vegetation and bare soils. Our vegetation map derives from MODIS satellite data (N. Viovy, personal communication, 2008). Our study domain reaches from 45°N to the North Pole, and all vegetation or bare soil patches are considered either tundra or taiga. At a model grid-cell scale, both environment types can coexist and cover a complementary fraction. Spatial variability of soil moisture is also accounted for at a subgrid scale [de Rosnay, 1999; Gouttevin et al., 2011], based on the soil texture map by Zobler [1986]. The soil thermal dynamics are computed separately for each environmental fraction. At the scale of the grid cell, soil in-depth and surface temperatures are then computed as the area-weighted averages of the environment-type-dependent temperatures.

3. Results

[12] Observed vertical profiles of snow density obtained at Barrow and Sodankylä in late March 2009 and 2010, i.e.,

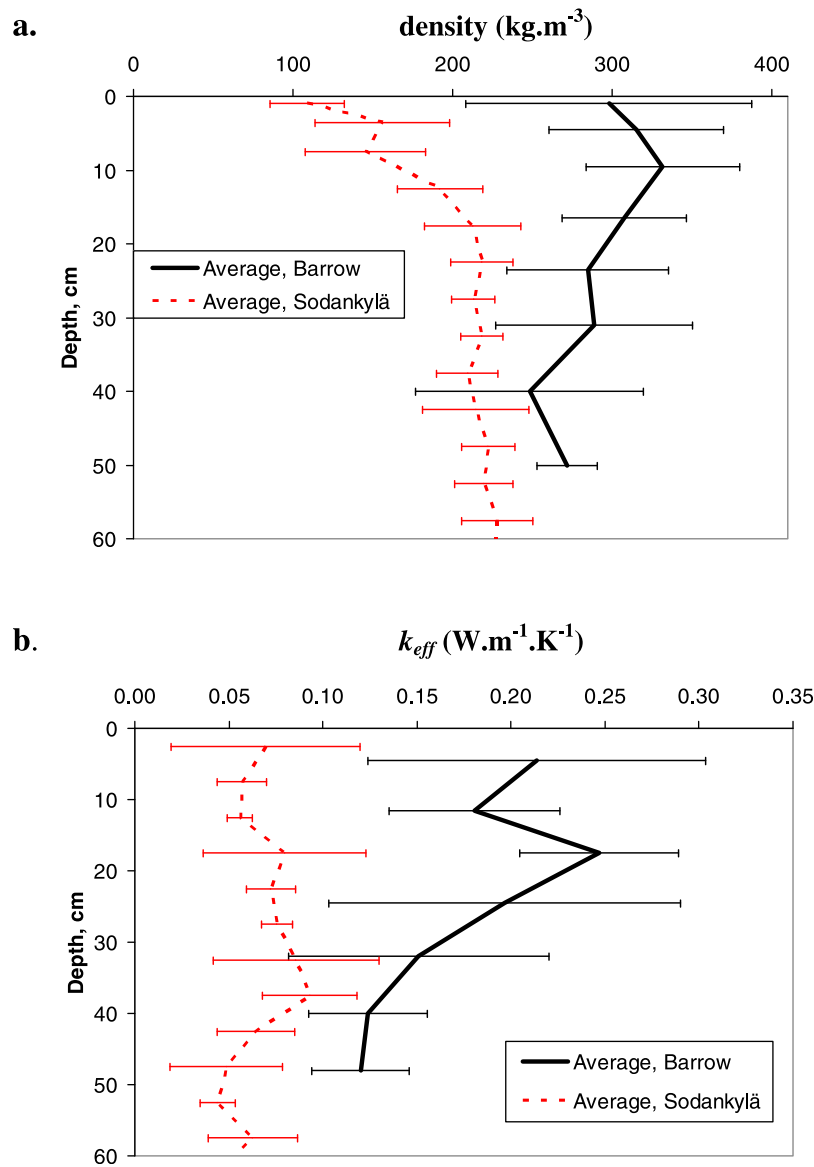


Figure 1. Average vertical profiles of (a) snow density and (b) thermal conductivity at Barrow, Alaska (71°N, typical tundra environment) and Sodankylä, Finnish Lapland (67°N, typical taiga environment). These averages are based on 7 profiles at Barrow and 8 profiles at Sodankylä. The error bars are the standard variations of the measurements. They are larger at Barrow because snow properties are affected by wind, and wind speed is very variable.

when the snowpack characteristics were established and before the onset of melting, are shown in Figure 1a. The average density around Barrow (7 profiles) is close to 300 kg m⁻³ while at Sodankylä (8 profiles) it is about 200 kg m⁻³. The average snow depth was 42 cm at Barrow, and 68 cm at Sodankylä. Thermal conductivity data is shown in Figure 1b. At Sodankylä, the average profile shows no trend with height and the average value is 0.07 W m⁻¹ K⁻¹. At Barrow, the top windpack layers have values in the range 0.2 to 0.25 W m⁻¹ K⁻¹, while the basal depth hoar layers have values around 0.15 W m⁻¹ K⁻¹. The interest of these data is that they represent unique simultaneous ρ and k_{eff} vertical profiles in two typical environments relevant to our study.

[13] Our measurements are not necessarily representative of the whole Subarctic and Arctic environments, nor of

the whole snow season. Based on other isolated measurements obtained by us and others [Sturm and Johnson, 1992; Taillandier et al., 2006; Dominé et al., 2011], we estimate that our taiga values are probably well representative of the general taiga environment, which remains very insulative for the whole snow season. We will therefore use (200, 0.07) as representative (ρ , k_{eff}) values for taiga (Table 1). For tundra, the absence of strong wind storms at Barrow in 2009 when our measurements were made (F. Dominé et al., Physical properties of the Arctic snowpack during OASIS, submitted to *Journal of Geophysical Research*, 2011) prevented the formation of hard dense windpacks with high k_{eff} frequently found elsewhere [Sturm et al., 1997; Dominé et al., 2002, 2011; Derksen et al., 2009], and also probably resulted in depth hoar softer than usual. Besides, our measurements

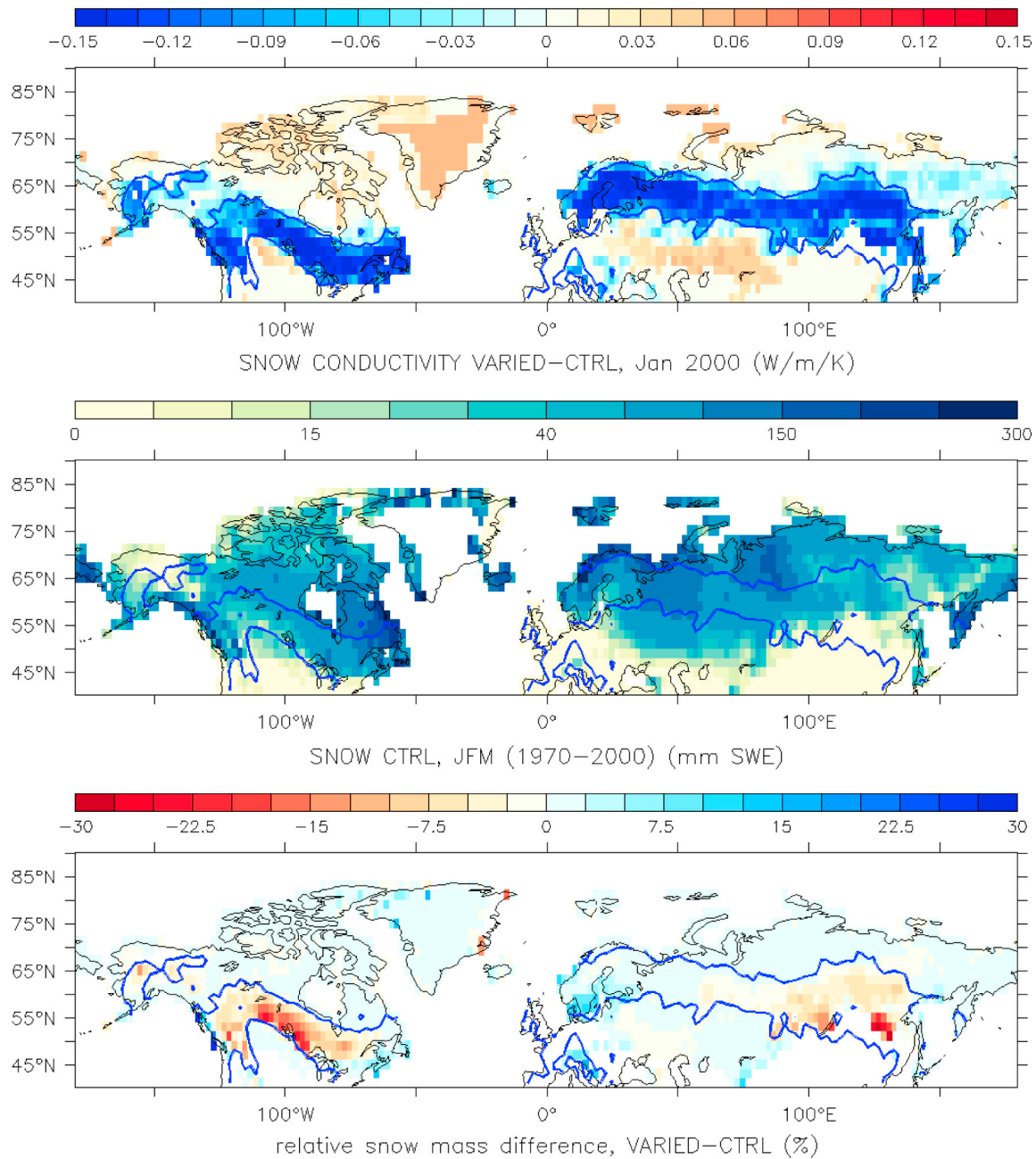


Figure 2. (top) Snow conductivity difference between the simulations VARIED and CTRL, averaged over the year 2000. In all maps, the blue line contours the areas where taiga environment covers more than 50% of the model grid-cell. (middle) Mean winter snow water equivalent (SWE) in the CTRL simulation over 1970–2000. (bottom) Relative SWE difference between the simulations VARIED and CTRL over 1970–2000.

describe an end-of-the-season snowpack where basal depth hoar had time to develop: earlier in the season, tundra snowpack mostly consists of dense and conductive wind-slabs. Therefore we estimate that typical (ρ, k_{eff}) values for tundra snow are rather (330, 0.25), which we will use subsequently (Table 1). Our snow density values for tundra and taiga environments are in good agreement with values recurrently found in literature [Sturm *et al.*, 1995; Derksen *et al.*, 2009].

[14] Unless otherwise stated, the comparisons performed and analyzed in this section involve the results of the CTRL and VARIED simulations for the 1970–2000 period, a 30-year span filtering interannual variability. Differences between the two simulations correspond to VARIED minus CTRL. Winter refers to the period between January and March; summer encompasses July to September. Figure 2 (top) illustrates the prescribed spatial changes in snow thermal conductivity between the VARIED and CTRL simulations. The calculated snow conductivity is an average

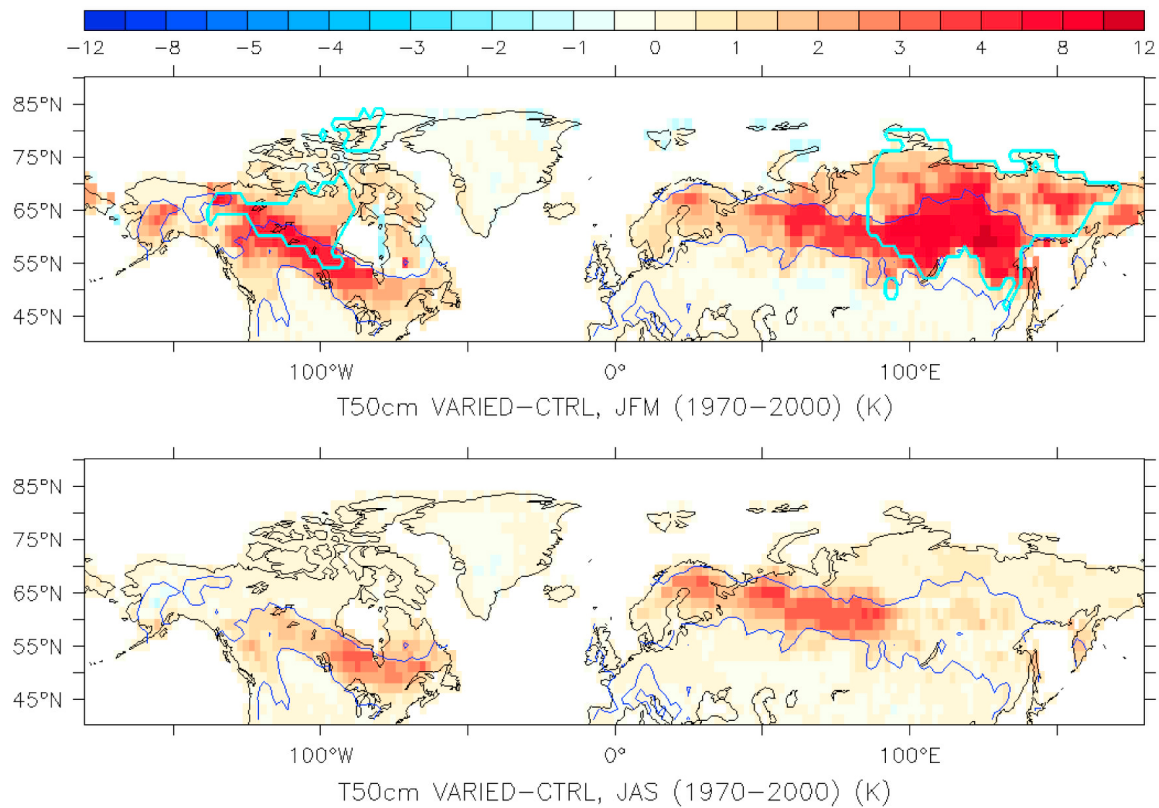


Figure 3. A 50-cm soil temperature difference between the VARIED and CTRL simulations for the period 1970–2000, over the months of (top) January to March and (bottom) July to September. The light-blue line contours areas exhibiting a >40 K annual thermal amplitude and a >5 mm snow water equivalent in winter.

conductivity, weighted by the areas of tundra and taiga over the grid-cell. The changes of highest magnitude correspond to the Fennoscandian and Canadian taiga belts, as outlined by the blue contours. However, a reduction in snow thermal conductivity is also computed for regions of sparse tree or shrub-like vegetation at the extent of the Siberian Kolyma region. This is a consequence of the very low value of snow conductivity chosen for taiga environment, which enhances the impact of sparse vegetation at the grid-cell scale. The averaged winter snow cover depth and its variation between the CTRL and VARIED simulations are illustrated in Figure 2 (middle and bottom); CTRL and VARIED simulations exhibit moderate snow depth differences (up to 10 cm, i.e., 20% less SWE in the VARIED simulation in the North American taiga belt) imputable to higher sublimation and melting rates triggered by increased soil temperatures.

[15] Figure 3 displays the difference in 50-cm soil temperature between the simulations VARIED and CTRL over winter (top) and summer (bottom). The use of a reduced snow conductivity yields warmer topsoil temperatures in taiga-dominated regions in winter (Figure 3, top). The soil temperature difference between VARIED and CTRL can amount to up to 12 K at 50 cm depth in the soil. This means a thermal offset of about this magnitude between air temperature and snow-soil interface temperature in the taiga areas of the VARIED simulation, which is supported by observations [e.g., Sullivan *et al.*, 2008]. The difference map exhibits very specific spatial characteristics. First, it is not

restricted to areas where the taiga fraction exceeds 50% (Figure 3, blue contours) and not even to areas where the grid-cell-averaged snow conductivity is reduced upon the use of an ecosystem-type-dependent snow conductivity. For instance, the grid-cell-averaged snow thermal conductivity over the Taymyr peninsula is increased in the VARIED simulation; this region is nevertheless subject to winter warming when compared to the CTRL simulation (Figure 3, top). This illustrates the nonlinearity of snow and soil thermal dynamics with respect to thermal characteristics: the warming effect of taiga snow on minor isolated vegetation patches can dominate the grid-cell-averaged temperature difference between VARIED and CTRL over the cooling induced by the dominant tundra snow cover. The second characteristic of the winter soil temperature difference is the spatial pattern of its peak magnitude over the East Siberian and North American taiga regions. This pattern mainly results from the combination of high annual thermal amplitudes and sufficient insulative snow cover (Figure 3, top). High annual thermal amplitudes indeed enhance the impact of snow insulation: upon a perfect thermal insulation over winter, the soil would keep its thermal summer state. Therefore, the winter soil temperature difference with minus without insulation would roughly equal the annual thermal amplitude between the two seasons. The winter thermal signal correlates only weakly with the winter snow depth (Figure 2, middle) or snow duration (not shown).

[16] The summer soil temperatures are also of importance for our study since most of the soil microbial activity takes

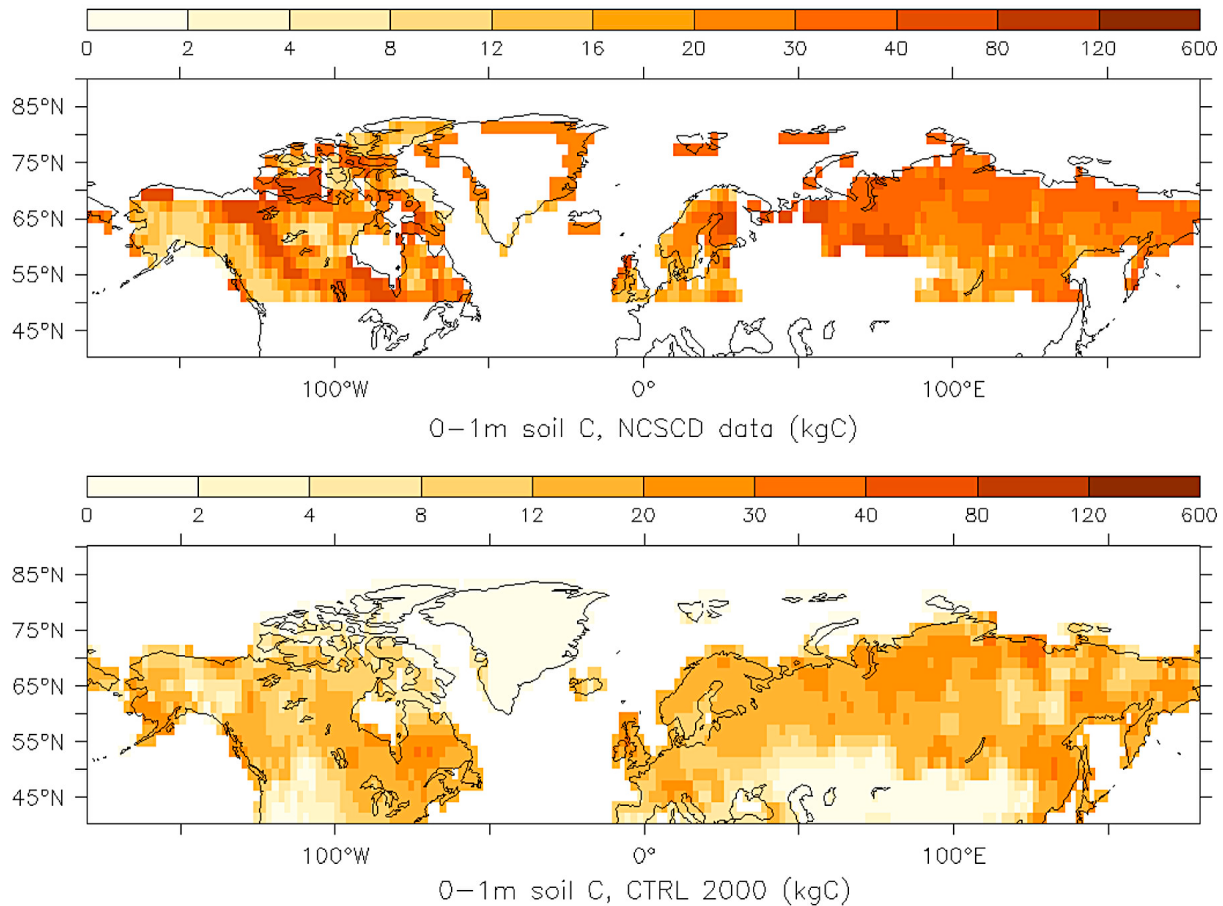


Figure 4. Soil carbon stocks in the uppermost meter of the soil, (top) as estimated by the NCSCD and (bottom) as simulated by ORCHIDEE after a 10,000-year buildup in the CTRL simulation.

place during this season when part of the soil has temperatures above the melting point. In most high latitude regions the winter higher temperatures induced by the change in snow conductivity persists over summer (Figure 3, bottom). However, the peak amplitudes are reduced (~ 4 K) and the spatial pattern is very different: the strongest summer warming is modeled in the taiga areas that received a quite thick snow cover during the preceding winter (>60 cm); in those regions the snow cover also lasts more than 6 months.

[17] Overall, the use of ecosystem-differentiated snow thermal properties yields more realistic soil temperatures, partially correcting the model's systematic cold bias reported by other studies [Koven *et al.*, 2009; Gouttevin *et al.*, 2011]. As an illustration, the model versus data RMS error in soil temperatures at HRST stations [Zhang *et al.*, 2001] for the decade (1984–1994) is reduced by 2 K in the VARIED simulation (Figure S1).¹

[18] The soil carbon dynamics are very sensitive to soil temperatures, both in the model and in reality, and the thermal signal resulting from changes in the snow cover characteristics affects the soil carbon stocks and fluxes. Figure 4 compares the carbon stocks of the first meter of the soil as simulated by the CTRL simulation, and as estimated by the Northern Circumpolar Soil Carbon Database (NCSCD)

[Tarnocai *et al.*, 2009] on the basis of pedon samples. The simulated carbon stocks underestimate the amount of carbon inferred from the in situ measurements for the uppermost 3 m of the soil (1024 PgC according to Tarnocai *et al.* [2009], a value that may be lessened according to revised estimates by Schirrmeister *et al.* [2011], versus 872 PgC in our study). We insist that the NCSCD database relies on about 3 530 pedon samples with uneven spatial distribution and depth sampling. Confidence levels are high for North American uppermost soil meter but low to medium (33%–66%) for Siberian uppermost soils and even lower ($<33\%$) for deeper soil layers [Tarnocai *et al.*, 2009]. Part of our underestimation occurs because we do not explicitly model the buildup of peatlands or organic soils, which is especially noticeable in the Mackenzie region. On the other hand, an excessive productivity at high latitudes is a known bias of our model and partially offsets this structural carbon deficit [Beer *et al.*, 2010; Koven *et al.*, 2011]. Despite the simplified spinup procedure and inaccurate description of complex circumpolar pedogenesis, the model manages to capture the spatial features of the high latitude soil carbon stocks, for instance the high soil carbon content of the Archangelsk region, West Siberian lowlands, lower Lena basin and Chukotka.

[19] The use of ecosystem-differentiated snow thermal properties has a global impact on the modeled soil carbon stocks (Figure 5a). A reduction of the soil carbon stock is

¹Auxiliary materials are available in the HTML. doi:10.1029/2011JG001916.

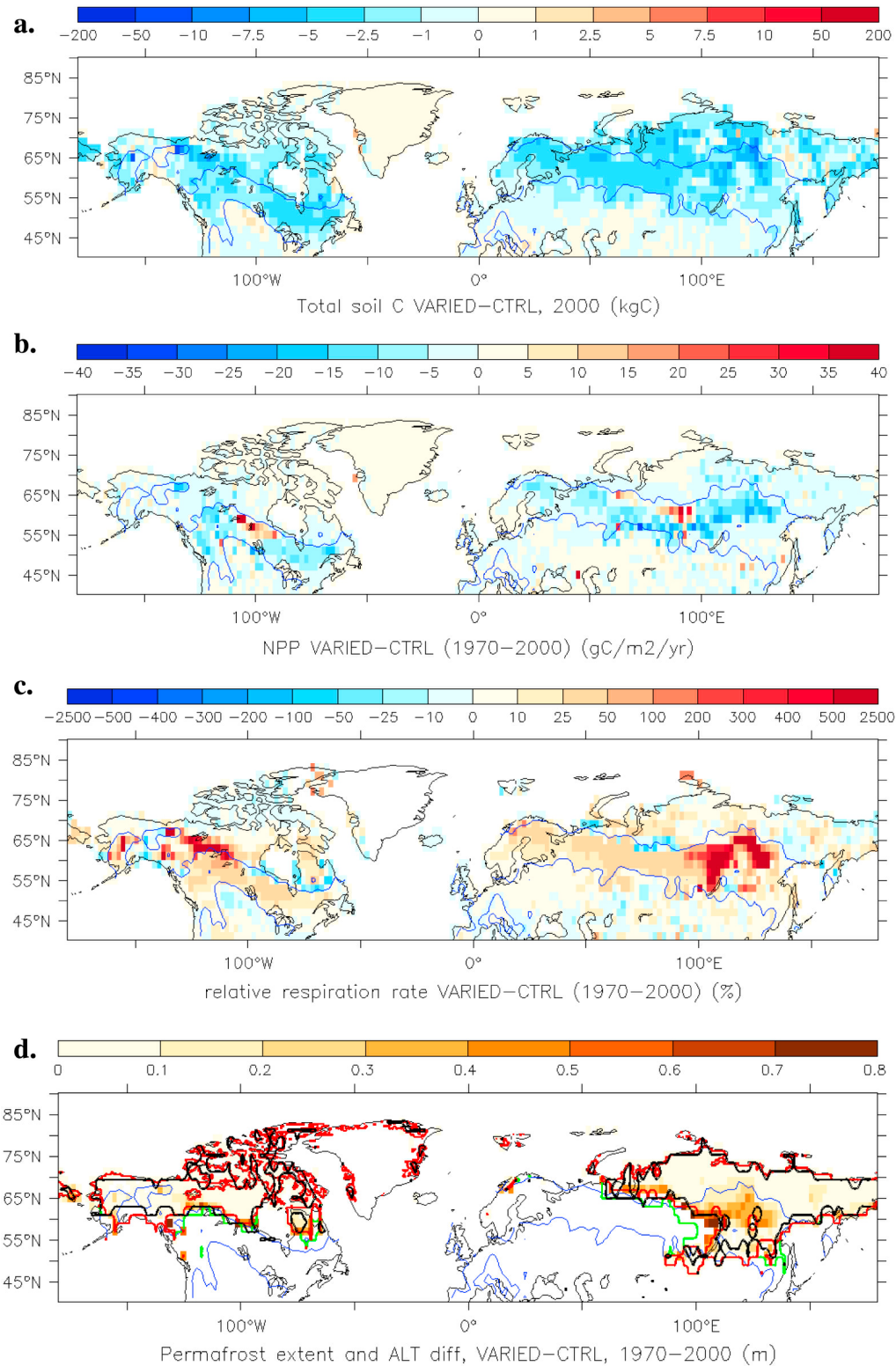


Figure 5. Soil carbon stocks differences and explanatory variables. (a) Total soil carbon stock difference between the VARIED and CTRL simulations after 10,000 years of model spinup. (b) Average net primary production (NPP) difference. (c) Relative respiration rate difference. (d) Permafrost extent and active layer thickness difference in remaining permafrost areas. Green, red and black lines respectively contour the permafrost extent by year 2000 (continuous + discontinuous) as simulated in the CTRL configuration, in the VARIED configuration, and as compiled by the International Permafrost Association [Brown *et al.*, 1998]. Where no green line is seen, VARIED and CTRL permafrost contours coincide.

simulated over most of the Arctic, with an enhanced magnitude in regions subject to (i) strong summer warming (Fennoscandian taiga); (ii) summer warming and exhibiting very large carbon contents (lower Ienissei and Lena basins); (iii) summer warming and permafrost disappearance or active layer increase (Iakutia, Evenkia; Figure 5d). The total modeled difference in soil carbon stocks amounts to 64 PgC, or 8% of the modeled carbon stocks. Where carbon stocks are particularly high (lower Ienissei region), less than 0.5 K summer warming is enough to trigger a strong shift in the local carbon balance, reflected by differences in carbon stock amounts ($>2.5 \text{ kg/m}^2$).

[20] The carbon stocks difference between the VARIED and CTRL simulations result from changes in the soil and biomass carbon dynamics. We here successively analyze the changes in soil carbon inputs and outputs driving this difference. Overall, forest plant functional types are more productive in Central Siberia and Central Canada in the VARIED simulation: there, ecosystems are nitrogen limited [Friedlingstein *et al.*, 1999], a constraint which is loosened by warmer all-year (and especially spring and summer) soil temperatures at the southern permafrost margins (Figure 3). On the opposite, non-tree plant functional types tend to be overall less productive in the VARIED simulation especially in areas with enhanced tree productivity: this results from a combination of increased light limitation and, locally, enhanced surface water stress induced by warmer summer soil temperatures. Though the resulting spatial pattern of net primary production difference is heterogeneous (Figure 5b), net primary production is overall decreased between VARIED and CTRL ($\sim -0.06 \text{ PgC/yr}$ over our study area).

[21] In terms of soil carbon outputs, heterotrophic respiration is stimulated by higher soil temperatures in the VARIED simulation, as reflected by higher soil respiration rates (Figure 5c; +22% increase in respiration rate over our study area). Where permafrost is lost or active layer is deepened in the VARIED simulation (Iakutia and Evenkia), a significant increase in the relative respiration rate is modeled: whereas carbon is stored in the perennially frozen soils of the CTRL simulation, it undergoes microbial decomposition in the VARIED simulation (Figures 5c–5d). In the Fennoscandian taiga, higher insulation by snow in the VARIED simulation leads to winter soil temperatures close to the freezing point: organic matter decomposition thus occurs below the snow cover. This winter soil respiration contributes to an average of 30%, but locally up to 50%, of the modeled difference in annual respiration rates between the two simulations (Figure S2). The combined effects of globally reduced net primary productivity and increased respiration rates in the VARIED simulation result in the net soil carbon stocks difference between the VARIED and CTRL simulations (Figure 5a).

[22] Finally, the ecosystem-differentiated description of snow yields an improvement in the modeled permafrost extent (Figure 5d) based on in situ data compiled by the International Permafrost Association [Brown *et al.*, 1998]. In particular, the central Siberian permafrost-free region is very well captured by the VARIED simulation, indicating that the recurrent cold bias of models in this region [Dankers *et al.*, 2011] may originate from a coarse description of snow insulation. In our simulations, permafrost is defined as the area where at least one soil layer remains below the freezing

point from one year to another. Assuming a spatially Gaussian temperature distribution at the scale of the grid-cell, this threshold ensures that an annually frozen layer underlies more than 50% of the grid-cell area. It thus characterizes the continuous and discontinuous permafrost as defined by the International Permafrost Association, which is the basis for our comparison. Our modeled extents are 18.1 M km^2 in the CTRL simulation and 15.9 M km^2 in the VARIED simulation. The latter extent compares reasonably well to the latest estimates of 15.7 M km^2 by Zhang *et al.* [2008] for continuous and discontinuous permafrost.

4. Discussion and Conclusion

[23] Our study is a model-based illustration of the crucial role of insulation by snow in the soil thermal regime and in the processes involved in the formation and decomposition of soil organic matter. The mere representation of differentiated snow thermal properties for two complementary Arctic ecosystems yields notable differences in the repartition and amount of current terrestrial carbon: soil carbon decomposition is enhanced upon winter warming close to the freezing point, higher summer temperatures, thicker active layers and reduced permafrost extent. The current permafrost zonation is thus captured with more accuracy.

[24] We underline that measurements performed in late March, as made for this study and retrieved from the cited literature [Derksen *et al.*, 2009] possibly underestimate the thermal conductivity difference between our two snow types of interest. Taiga snow remains poorly conductive during the whole snow season, as it mainly consists out of recent snow and depth hoar [Sturm *et al.*, 1995]. On the opposite, fresh snow is rare on the tundra and rapidly transforms into windslabs of high k_{eff} . The thermal resistance of the tundra snowpack is higher at the end of the snow season as windslabs partially transformed into depth hoar [Derksen *et al.*, 2009]. Hence the real thermal effect of the different snow properties might be underestimated in our study.

[25] Distinguishing between taiga and tundra snow is a first step toward an improved representation of the snow and soil thermal regime in land-surface models. More detailed snow classifications exist [Sturm *et al.*, 1995]. The snow classes identified exhibit fairly different thermal characteristics and can be retrieved from climatic conditions, hence their potential for use in land-surface or climate modeling. Our study focused on the effects induced by the two dominant snow classes of the northern circumpolar area. Further experiments could involve an increased degree of refinement in the description and mapping of the snow cover thermal properties.

[26] Also, our snow model is very coarse, which limited our ability to explore in this study more realistic spatial distributions of snow properties. Current developments (discussed in T. Wang *et al.*, Evaluation of ORCHIDEE snow model using point observations at SNOWMIP sites and regional snow observations, manuscript in preparation, 2012) aim at representing a vertical and horizontal variability in snow properties, and account for interactions with the canopy. They should provide a new tool to produce a refined estimate of the effects investigated by this study.

[27] Shrub expansion and northward migration of the tree line at the pan-Arctic scale have been reported over the past

three decades [Serreze *et al.*, 2000; Sturm *et al.*, 2001b; Jia *et al.*, 2003; Tape *et al.*, 2006; Forbes *et al.*, 2010], in link with recent climate warming. These ecosystem changes have been shown to affect the local and global climate conditions [Sturm *et al.*, 2001a, 2005a; Lawrence and Swenson, 2011] as well as carbon cycling at high latitudes [Sullivan, 2010]. Diverse and intricate processes are at stake, at the instance of changes in albedo and surface roughness shifting the partitioning of energy between surface and atmosphere, changes in evapotranspiration, soil moisture regime, shading, but also snow trapping and distribution. These processes have also been shown to possibly sustain further shrub growth through soil biological feedback [Sturm *et al.*, 2005b] and enhance soil carbon loss [Sullivan, 2010].

[28] Still, the implications of these changes in the global context are hard to assess: using the CLM model, Lawrence and Swenson [2011], for instance, inferred greater active layer thicknesses under shrubs in an idealized pan-Arctic +20% shrub-area experiment. However, this result could be balanced by considering snow redistribution processes. Here, the specific snow metamorphism and snow thermal properties pertaining to forested areas are highlighted as a further feedback mechanism, which bears consequences for biogeochemical cycling in the Arctic and therefore for global climate.

[29] The intrication of the processes involved makes a complete physical modeling of land surface processes paramount in the prospect of reliable climate projections. A detailed snow modeling is part of it and should not be left out as it entails substantial climatic implications. We hope that our study will foster model developments considering the tied evolution of snow, vegetation and high latitude soil carbon in a changing climate.

[30] **Acknowledgments.** The modeling work was supported by funding from the European Union 7th Framework Programme under projects Page21 (grant 282700), Combine (grant 226520), and LIFE SNOWCARBO. The fieldwork in Barrow was funded by the French Polar Institute (grant 1017). The fieldwork in Sodankylä was funded by the Programme National de Télédétection Spatiale of CNRS as part of the SNORTEX campaign. FD thanks J.-L. Roujean for his invitation to SNORTEX. We thank the Editor, Associate Editor and anonymous reviewers for their relevant comments, which helped to refine our study and improve the manuscript.

References

- Alexeev, V., D. Nicolsky, V. Romanovsky, and D. Lawrence (2007), An evaluation of deep soil configurations in the CLM3 for improved representation of permafrost, *Geophys. Res. Lett.*, **34**, L09502, doi:10.1029/2007GL029536.
- Beer, C., et al. (2010), Terrestrial Gross Carbon Dioxide Uptake: Global Distribution and Covariation with Climate, *Science*, **329**, 834–838, doi:10.1126/science.1184984.
- Brown, J., O. J. Ferrians Jr., J. A. Heginbottom, and E. S. Melnikov (1998), Circum-Arctic Map of Permafrost and Ground-Ice Conditions, <http://nsidc.org/data/ggd318.html>, Natl. Snow and Ice Data Cent./World Data Cent. for Glaciol, Boulder, Colo. [Revised Feb. 2001.].
- Chalita, S. (1992), Sensibilité du modèle de circulation atmosphérique LMD à l'albédo des surfaces enneigées, PhD thesis, Paris VI Univ., Paris.
- Christensen, T. R., T. Johansson, H. J. Akerman, M. Mastepanov, N. Malmer, T. Friberg, P. Crill, and B. H. Svensson (2004), Thawing sub-arctic permafrost: Effects on vegetation and methane emissions, *Geophys. Res. Lett.*, **31**, L04501, doi:10.1029/2003GL018680.
- Dankers, R., E. J. Burke, and J. Price (2011), Simulation of permafrost and seasonal thaw depth in the JULES land surface scheme, *The Cryosphere Discuss.*, **5**, 1263–1309, doi:10.5194/tcd-5-1263-2011.
- Davidson, E., and I. Janssens (2006), Temperature sensitivity of soil carbon decomposition and feedbacks to climate change, *Nature*, **440**, 165–173, doi:10.1038/nature04514.
- de Rosnay, P. (1999), Representation of soil-vegetation-atmosphere interaction in the general circulation model of the Laboratoire de Météorologie Dynamique, PhD thesis, Paris VI Univ., Paris.
- Derksen, C., A. Silis, M. Sturm, J. Holmgren, G. E. Liston, H. Huntington, and D. Solie (2009), Northwest Territories and Nunavut snow characteristics from a subarctic traverse: Implications for passive microwave remote sensing, *J. Hydrometeorol.*, **10**(2), 448–463, doi:10.1175/2008JHM1074.1.
- Dominé, F., A. Cabanes, and L. Legagneux (2002), Structure, microphysics, and surface area of the Arctic snowpack near Alert during the ALERT 2000 campaign, *Atmos. Environ.*, **36**(15–16), 2753–2765, doi:10.1016/S1352-2310(02)00108-5.
- Dominé, F., A. Taillandier, S. Houdier, F. Parrenin, W. Simpson, and T. Douglas (2007), Interactions between snow metamorphism and climate: Physical and chemical aspects, in *Physics and Chemistry of Ice*, edited by W. F. Kuhs, pp. 27–46, R. Soc. of Chem., Cambridge, UK.
- Dominé, F., J. Bock, S. Morin, and G. Giraud (2011), Linking the effective thermal conductivity of snow to its shear strength and its density, *J. Geophys. Res.*, **116**, F04027, doi:10.1029/2011JF002000.
- Forbes, B., M. Fauria, and P. Zetterberg (2010), Russian Arctic warming and “greening” are closely tracked by tundra shrub willows, *Global Change Biol.*, **16**, 1542–1554, doi:10.1111/j.1365-2486.2009.02047.x.
- Friedlingstein, P., G. Joel, C. B. Field, and I. Y. Fung (1999), Toward an allocation scheme for global terrestrial carbon models, *Global Change Biol.*, **5**, 755–770, doi:10.1046/j.1365-2486.1999.00269.x.
- Friedlingstein, P., et al. (2006), Climate-carbon cycle feedback analysis: Results from the C4MIP model intercomparison, *J. Clim.*, **19**, 3337–3353, doi:10.1175/JCLI3800.1.
- Ganopolski, A., S. Rahmstorf, V. Petoukhov, and M. Claussen (1998), Simulation of modern and glacial climates with a coupled global model of intermediate complexity, *Nature*, **391**, 351–356, doi:10.1038/34839.
- Gouttevin, I., G. Krinner, P. Ciais, J. Polcher, and C. Legout (2011), Multi-scale validation of a new soil freezing scheme for a land-surface model with physically based hydrology, *The Cryosphere Discuss.*, **5**, 2197–2252, doi:10.5194/tcd-5-2197-2011.
- Gruber, N., P. Friedlingstein, C. B. Field, R. Valentini, M. Heimann, J. E. Richey, P. Romero-Lankao, D. Schulze, and C.-T. A. Chen (2004), The vulnerability of the carbon cycle in the 21st century: An assessment of carbon-climate-human interactions, in *The Global Carbon Cycle: Integrating Humans, Climate, and the Natural World*, edited by C. B. Field and M. R. Raupach, pp. 45–76, Island Press, Washington, D. C.
- Jia, G., H. Epstein, and D. Walker (2003), Greening of arctic Alaska, 1981–2001, *Geophys. Res. Lett.*, **30**(20), 2067, doi:10.1029/2003GL018268.
- Kelley, J. J., D. F. Weaver, and B. P. Smith (1968), The variation of carbon dioxide under the snow in the Arctic, *Ecology*, **49**, 358–361, doi:10.2307/1934472.
- Khvorostyanov, D. V., P. Ciais, G. Krinner, S. Zimov, C. Corradi, and G. Guggenberger (2008), Vulnerability of permafrost carbon to global warming. Part II: Sensitivity of permafrost carbon stock to global warming, *Tellus, Ser. B*, **60**, 265–275, doi:10.1111/j.1600-0889.2007.00336.x.
- Kleinen, T., V. Brovkin, W. von Bloh, D. Archer, and G. Munhoven (2010), Holocene carbon cycle dynamics, *Geophys. Res. Lett.*, **37**, L02705, doi:10.1029/2009GL041391.
- Koven, C., P. Friedlingstein, P. Ciais, D. Khvorostyanov, G. Krinner, and C. Tarnocai (2009), On the formation of high-latitude soil carbon stocks: Effects of cryoturbation and insulation by organic matter in a land surface model, *Geophys. Res. Lett.*, **36**, L21501, doi:10.1029/2009GL040150.
- Koven, C., B. Ringeval, P. Friedlingstein, P. Ciais, P. Cadule, D. Khvorostyanov, G. Krinner, and C. Tarnocai (2011), Permafrost carbon-climate feedbacks accelerate global warming, *Proc. Natl. Acad. Sci. U. S. A.*, **108**(36), 14,769–14,774, doi:10.1073/pnas.1103910108.
- Krinner, G., N. Viovy, N. de Noblet-Ducoudré, J. Ogée, J. Polcher, P. Friedlingstein, P. Ciais, S. Sitch, and I. Prentice (2005), A dynamic global vegetation model for studies of the coupled atmosphere-biosphere system, *Global Biogeochem. Cycles*, **19**, GB1015, doi:10.1029/2003GB002199.
- Lawrence, D. M., and A. G. Slater (2010), The contribution of snow condition trends to future ground climate, *Clim. Dyn.*, **34**(7–8), 969–981, doi:10.1007/s00382-009-0537-4.
- Lawrence, D. M., and S. C. Swenson (2011), Permafrost response to increasing arctic shrub abundance depends on the relative influence of shrubs on local cooling versus large-scale warming, *Environ. Res. Lett.*, **6**, 045504, doi:10.1088/1748-9326/6/4/045504.
- Ling, F., and T. J. Zhang (2006), Sensitivity of ground thermal regime and surface energy fluxes to tundra snow density in northern Alaska, *Cold Reg. Sci. Technol.*, **44**(2), 121–130, doi:10.1016/j.coldregions.2005.09.002.
- Meehl, G. A. et al. (2007), Global climate projections, in *Climate Change 2007: The Physical Science Basis. Contribution of Working Group I to the Fourth Assessment Report of the Intergovernmental Panel on Climate*

- Change*, edited by S. Solomon et al., pp. 789–844, Cambridge Univ. Press, Cambridge, U. K.
- Mitchell, T. D., and P. D. Jones (2005), An improved method of constructing a database of monthly climate observations and associated high resolution grids, *Int. J. Climatol.*, **25**, 693–712, doi:10.1002/joc.1181.
- Morin, S., F. Dominé, L. Arnaud, and G. Picard (2010), In-situ measurement of the effective thermal conductivity of snow, *Cold Reg. Sci. Technol.*, **64**, 73–80, doi:10.1016/j.coldregions.2010.02.008.
- Nobrega, S., and P. Grogan (2007), Deeper snow enhances winter respiration from both plant-associated and bulk soil carbon pools in birch hummock tundra, *Ecosystems* (N. Y.), **10**, 419–431, doi:10.1007/s10021-007-9033-z.
- Petoukhov, V., A. Ganopolski, V. Brovkin, M. Claussen, A. Eliseev, C. Kubatzki, and S. Rahmstorf (2000), CLIMBER-2: A climate system model of intermediate complexity. Part I: Model description and performance for present climate, *Clim. Dyn.*, **16**, 1–17, doi:10.1007/PL00007919.
- Qian, B., E. Gregorich, S. Gameda, D. Hopkins, and X. Wang (2011), Observed soil temperature trends associated with climate change in Canada, *J. Geophys. Res.*, **116**, D02106, doi:10.1029/2010JD015012.
- Randall, D. A., et al. (2007), Climate models and their evaluation, in *Climate Change 2007: The Physical Science Basis. Contribution of Working Group I to the Fourth Assessment Report of the Intergovernmental Panel on Climate Change*, edited by S. Solomon et al., pp. 589–662, Cambridge Univ. Press, Cambridge, U. K.
- Schaphoff, S., W. Lucht, D. Gerten, S. Sitch, W. Cramer, and I. Prentice (2006), Terrestrial Biosphere carbon storage under alternative climate projections, *Clim. Change*, **74**, 97–122, doi:10.1007/s10584-005-9002-5.
- Schirmermeister, L., C. Siegert, T. Kuznetsova, S. Kuzmina, A. Andreev, F. Kienast, H. Meyer, and A. Bobrov (2002), Paleoenvironmental and paleoclimatic records from permafrost deposits in the Arctic region of Northern Siberia, *Quat. Int.*, **89**, 97–118, doi:10.1016/S1040-6182(01)00083-0.
- Schirmermeister, L., G. Grosse, S. Wetterich, P. P. Overduin, J. Strauss, E. A. G. Schuur, and H.-W. Hubberten (2011), Fossil organic matter characteristics in permafrost deposits of the northeast Siberian Arctic, *J. Geophys. Res.*, **116**, G00M02, doi:10.1029/2011JG001647.
- Schuur, E. A. G., et al. (2008), Vulnerability of permafrost carbon to climate change: Implications for the global carbon cycle, *BioScience*, **58**, 701–714, doi:10.1641/B580807.
- Schuur, E. A. G., J. G. Vogel, K. G. Crummer, H. Lee, J. O. Sickman, and T. E. Osterkamp (2009), The effect of permafrost thaw on old carbon release and net carbon exchange from tundra, *Nature*, **459**, 556–559, doi:10.1038/nature08031.
- Serreze, M., J. Walsh, F. Chapin, T. Osterkamp, M. Dyurgerov, V. Romanovsky, W. Oechel, J. Morison, T. Zhang, and R. Barry (2000), Observational evidence of recent change in the northern high-latitude environment, *Clim. Change*, **46**, 159–207, doi:10.1023/A:1005504031923.
- Sturm, M., and J. Johnson (1992), Thermal conductivity measurements of depth hoar, *J. Geophys. Res.*, **97**(B2), 2129–2139, doi:10.1029/91JB02685.
- Sturm, M., J. Holmgren, and G. E. Liston (1995), A seasonal snow cover classification system for local to global applications, *J. Clim.*, **8**, 1261–1283, doi:10.1175/1520-0442(1995)008<1261:ASSCCS>2.0.CO;2.
- Sturm, M., J. Holmgren, M. König, and K. Morris (1997), The thermal conductivity of seasonal snow, *J. Glaciol.*, **43**(143), 26–41.
- Sturm, M., J. McFadden, G. E. Liston, F. Chapin III, C. Racine, and J. Holmgren (2001a), Snow-shrub interactions in Arctic tundra: A hypothesis with climatic implications, *J. Clim.*, **14**, 336–344, doi:10.1175/1520-0442(2001)014<0336:SSIIAT>2.0.CO;2.
- Sturm, M., C. Racine, and K. Tape (2001b), Increasing shrub abundance in the Arctic, *Nature*, **411**, 546–547, doi:10.1038/35079180.
- Sturm, M., T. Douglas, C. Racine, and G. E. Liston (2005a), Changing snow and shrub conditions affect albedo with global implications, *J. Geophys. Res.*, **110**, G01004, doi:10.1029/2005JG000013.
- Sturm, M., J. Schimel, G. Meachaelson, J. M. Welker, S. F. Oberbauer, G. E. Liston, J. Fahnestock, and V. E. Romanovsky (2005b), Winter biological processes could help convert Arctic tundra to shrubland, *BioScience*, **55**(1), 17–26, doi:10.1641/0006-3568(2005)055[0017:WBPHCH]2.0.CO;2.
- Sullivan, P. F. (2010), Snow distribution, soil temperature and late winter CO₂ efflux from soils near the Arctic treeline in northwest Alaska, *Biogeochemistry*, **99**, 65–77, doi:10.1007/s10533-009-9390-0.
- Sullivan, P. F., J. M. Welker, S. J. T. Arens, and B. Sveinbjörnsson (2008), Continuous estimates of CO₂ efflux from arctic and boreal soils during the snow-covered season in Alaska, *J. Geophys. Res.*, **113**, G04009, doi:10.1029/2008JG000715.
- Taillandier, A. S., F. Dominé, W. R. Simpson, M. Sturm, T. A. Douglas, and K. Severin (2006), Evolution of the snow area index of the subarctic snowpack in central Alaska over a whole season: Consequences for the air-to-snow transfer of pollutants, *Environ. Sci. Technol.*, **40**(24), 7521–7527, doi:10.1021/es060842j.
- Tape, K., M. Sturm, and C. Racine (2006), The evidence for shrub expansion in northern Alaska and the Pan-Arctic, *Global Change Biol.*, **12**, 686–702, doi:10.1111/j.1365-2486.2006.01128.x.
- Tarnocai, C., J. G. Canadell, E. A. G. Schuur, P. Kuhry, G. Mazhitova, and S. Zimov (2009), Soil organic carbon pools in the northern circumpolar permafrost region, *Global Biogeochem. Cycles*, **23**, GB2023, doi:10.1029/2008GB003327.
- Walker, M. D., et al. (1999), Long-term experimental manipulation of winter snow regime and summer temperature in arctic and alpine tundra, *Hydrol. Processes*, **13**, 2315–2330, doi:10.1002/(SICI)1099-1085(199910)13:14/15<2315::AID-HYP888>3.0.CO;2-A.
- Welker, J. M., J. M. Fahnestock, and M. H. Jones (2000), Annual CO₂ flux in dry and moist Arctic tundra: Field responses to increases in summer temperatures and winter snow depth, *Clim. Change*, **44**, 139–150, doi:10.1023/A:1005555012742.
- Westermann, S., J. Lüers, M. Langer, K. Piel, and J. Boike (2009), The annual surface energy budget of a high-Arctic permafrost site in Svalbard, Norway, *The Cryosphere*, **3**, 245–263, doi:10.5194/tc-3-245-2009.
- Zhang, T. (2005), Influence of the seasonal snow cover on the ground thermal regime: An overview, *Rev. Geophys.*, **43**, RG4002, doi:10.1029/2004RG000157.
- Zhang, T., R. Barry, and D. Gilichinsky (2001), Russian Historical Soil Temperature Data, <http://nsidc.org/data/arcs078.html>, Natl. Snow and Ice Data Cent., Boulder, Colo. [Updated 2006.]
- Zhang, T., R. Barry, K. Knowles, J. Heginbottom, and J. Brown (2008), Statistics and characteristics of permafrost and ground-ice distribution in the Northern Hemisphere, *Polar Geogr.*, **31**, 47–68, doi:10.1080/10889370802175895.
- Zhuang, Q. L., J. M. Melillo, M. C. Sarofim, D. W. Kicklighter, A. D. McGuire, B. S. Felzer, A. Sokolov, R. G. Prinn, P. A. Steudler, and S. M. Hu (2006), CO₂ and CH₄ exchanges between land ecosystems and the atmosphere in northern high latitudes over the 21st century, *Geophys. Res. Lett.*, **33**, L17403, doi:10.1029/2006GL026972.
- Zimov, S. A., G. M. Zimova, S. P. Daviodov, A. I. Daviodova, Y. V. Voropaev, Z. V. Voropaeva, S. F. Prosiannikov, O. V. Prosiannikova, I. V. Semiletova, and I. P. Semiletov (1993), Winter biotic activity and production of CO₂ in Siberian soils: A factor in the greenhouse effect, *J. Geophys. Res.*, **98**(D3), 5017–5023, doi:10.1029/92JD02473.
- Zimov, S., E. Schuur, and F. Chapin III (2006), Permafrost and the global carbon budget, *Science*, **312**, 1612–1613, doi:10.1126/science.1128908.
- Zobler, L. (1986), A world soil file for global climate modeling, *NASA Tech. Memo. 87802*, Goddard Space Flight Cent., Greenbelt, Md.